

Electronic Supplementary Information

**Enhancing Magnetoresistance in Tetrathiafulvalene Carboxylate
Modified Iron Oxide Nanoparticle Assemblies**

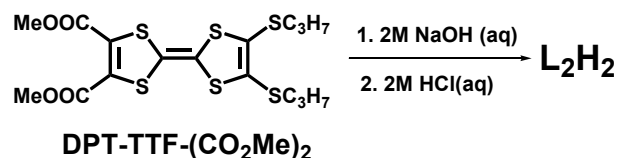
Zhong-Peng Lv,^a Zhong-Zhi Luan,^b Pei-Yu Cai,^a Tao Wang,^a Cheng-Hui Li,^a Di Wu,^b Jing-Lin Zuo*^a and Shouheng Sun*^c

^aState Key Laboratory of Coordination Chemistry, School of Chemistry and Chemical Engineering, Collaborative Innovation Center of Advanced Microstructures, Nanjing University, Nanjing 210093, P. R. China. Email: zuojl@nju.edu.cn

^bNational Laboratory of Solid State Microstructures, Department of Physics, Collaborative Innovation Center of Advanced Microstructures, Nanjing University, Nanjing 210093, P. R. China

^cDepartment of Chemistry, Brown University, Providence, Rhode Island 02912, USA. Email: ssun@brown.edu.

Synthesis of TTF-(COOH)₂, L₂H₂. The precursor compound DPT-TTF-(CO₂Me)₂ was synthesized according to the literature method.¹ Other reagents and solvents were purchased at reagent grade and used without further purification.



DPT-TTF-(CO₂Me)₂ (234 mg, 0.5 mmol) was dissolved in MeOH : THF (1:1/v:v) (25 mL). Then 2 M KOH aqueous solution (1.5 mL) was added. The solution was heated at reflux (80 °C) overnight. After the solvent removal, water was added and the solution was acidified to pH = 3 with 12 M HCl. The precipitate was collected by filtration and dried in vacuum to obtain L₂H₂ as a black purple powder (178 mg, 0.40 mmol, 80%). ¹H NMR (500 MHz, DMSO-*d*₆, δ) 2.89–2.79 (m, 4H, CH₂), 1.58 (h, *J* = 7.2 Hz, 4H, CH₂), 0.96 (t, *J* = 7.3 Hz, 6H, CH₃), no peak >10 ppm for COOH. ESI-MS *m/z*: calcd for C₃₁H₅₂O₂S₆ [M – H][–], 438.93; found 438.90.

Chemical Characterization. IR spectra of the KBr pellets of the NPs were recorded on a Bruker TENSOR 27 FT-IR spectrometer in transmission mode in the spectral range from 400 to 4000 cm^{–1} at a resolution of 1 cm^{–1} and 40 scans. ¹H-NMR spectra were collected on a Bruker AVANCE DRX-500 NMR spectrometer at room temperature. Mass spectra were recorded with a Thermo Fisher LCQ Fleet for ESI-MS. Elements were analyzed by energy dispersive X-ray (EDX) spectroscopy on a Hitachi S-4800 field emission scanning electron microscope (FE-SEM). The elemental mass percentage of Fe was determined by flame atomic absorption spectrometry (F-AAS) on a Hitachi 180-80 instrument.

Transmission Electron Microscopy (TEM). TEM and HRTEM images were acquired on a JEOL JEM 2100 microscope operated at 200 kV. The sample was prepared by evaporating a drop of hexane or chloroform dispersion of the NPs on a carbon-coated copper grid followed. Then, 6 pictures with in total 2240 particles were used to evaluate the particle size distribution of OA-NPs by image digitization software ImageJ. A bin size of 0.1 nm was chosen for the creation of the particle size histogram.

Small-angle X-ray Scattering (SAXS). Powder SAXS measurements were performed on an Anton Paar SAXSess mc2 instrument in the transmission mode using a Cu $K\alpha$ radiation ($\lambda = 0.15410$ nm) between the angles of 0.15° and 10° . The average NP interspace was calculated based on the length of the scattering vector $q = 4\pi \times \sin \theta / \lambda$ and Bragg equation $2d \times \sin \theta = \lambda$,

$$D_i = 2\pi / q_1 - 2\pi / q_2 \quad (2)$$

where D_i represents the average NP interspace, q_1 is the length of the scattering vector for the peak representing the average distance between the centers of two adjacent NPs, q_2 is the length of the scattering vector for the peak representing the average diameter of the NP cores.

Magnetization measurement. ZFC-FC curves and superparamagnetic hysteresis loops were obtained on a Quantum Design MPMS-SQUID-VSM magnetometer. The measured magnetic moment (emu) was then divided by the Fe_3O_4 mass (g) in the corresponding sample, which was the product of the sample mass and the mass percentage of Fe_3O_4 (**Table S3**), to obtain M (emu/g).

Electron-conduction and Magnetoresistance Testing. The $\rho_0-T^{-1/4}$, $I-V$, and MR-magnetic field curves were obtained from a home-built magnetic transportation measure system and multi-parameter physical properties measure system (PPMS). The NP powders were cold-pressed under pressure of 30 Mpa into pellets, which were connected to the PPMS by a gold wire via the conductive silver adhesive. The specific resistance ρ is expressed as

$$\rho = (R \times S) / L \quad (3)$$

where R is the resistance, S is the cross section area (herein we use the area of the gold film on each size), L is the thickness of the pellet.

The temperature dependent zero-bias resistivity ρ_0 of each sample was measured by applying a constant current and corrected from the linear region of the $I-V$ curve at different temperature points. MR ratio under a specific magnetic field (H) is expressed as

$$\text{MR}(H) = (\rho_H - \rho_0) / \rho_0 \quad (4)$$

where ρ_H is the specific resistance of the sample in the H , ρ_0 is the specific resistance of the sample in a zero-field. For most of the measurements the voltage was tuned to obtain $0.01 \mu\text{A}$ current for comparison.

Supplementary Figures and Tables

Table S1. Assignment of the main absorption peaks^a in the IR spectra of L₁H, L₂H₂, and the corresponding Fe₃O₄ NPs.

mode assignment	L ₁ H	L ₁ -Fe ₃ O ₄ NPs	L ₂ H ₂	L ₂ -Fe ₃ O ₄ NPs
ν C–H	2959 m	2959 m	2963 w	2960 w
	2931 m	2923 m	2928 w	2923 w
	2868 w		2868 w	
		2852 w		2852 w
ν C=O and	1677 s		1685 m	
		1618 w		1601 s
ν C–O	1299 s		1235 s	
		1386 s		1378 s
ν C=C	1563 m	1561 m	1556 m	1562 m
	1532 m	1531 m	1521 s	1533 m
δ CH ₂	1458 w	1457 w	1460 m	1456 w
δ O–H	1430 m		1415 m	
δ CH ₃	1378 m	---- ^b	1375 m	---- ^b
δ S–CH ₂	1291 m	1291 m	1292 m	1291 w
	1238 w	1234 w	---- ^b	1234 w
ν S–C–S	1042 w	1047 w	1059 w	1044 w
	888 w	887 w	883 w	884 w
Fe–O lattice		800–500 s,br		800–500 s,br

a Unit: cm⁻¹; s: strong; m: middle; w: weak, br: broad.

b Peaks that cannot be discerned due to other intense peaks coverage.

Table S2. Atomic percentage^a of the main elements in L₁-Fe₃O₄ NPs and L₂-Fe₃O₄ NPs.

	C	O	S	N	Fe
L ₁ -Fe ₃ O ₄ NPs	40.52	31.55	8.52	0.00	19.40
L ₂ -Fe ₃ O ₄ NPs	40.12	34.17	7.90	0.00	17.80

^a Only C, O, S, N and Fe are included and the sum of their percentage is 100%.

Table S3. Mass percentages of Fe, Fe₃O₄ and the organic layer^a in L₁-Fe₃O₄ and L₂-Fe₃O₄ NPs, as well as COO-binding density^b.

	$m(\text{Fe})$ (wt%)	$m(\text{Fe}_3\text{O}_4)$ (wt%)	$m(\text{L})$ (wt%)	n (1/nm ²) ^b
L ₁ -Fe ₃ O ₄ NPs	61.5	84.9	15.1	1.36
L ₂ -Fe ₃ O ₄ NPs	61.1	84.3	15.7	1.27

a The mass percentage of Fe₃O₄ is converted from the mass percentage of Fe determined by F-AAS. The mass of organic layer $m(\text{L})$ equals to $1 - m(\text{Fe}_3\text{O}_4)$.

b The grafting density n is obtain by assuming a uniform 5.7 nm diameter and 5.2 g/cm³ density for a sphere Fe₃O₄ core.

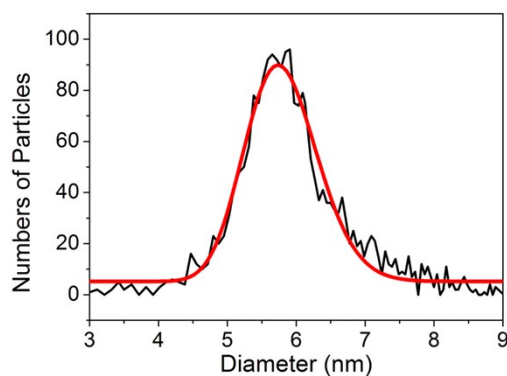


Fig. S1. Size distribution of the diameter of the Fe₃O₄ NP cores obtained from TEM measurements (black curve). The distribution is fitted using a log-normal distribution function (red curve). Accordingly, the average diameter of the Fe₃O₄ NP cores is 5.7 ± 0.6 nm.

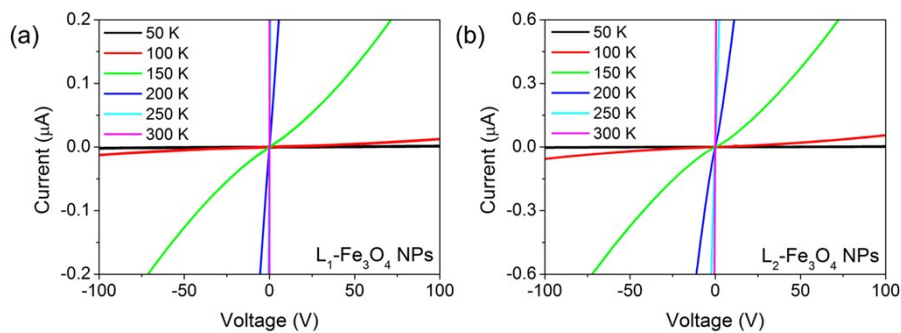


Fig. S2. I - V curves of (a) L₁-Fe₃O₄ and (b) L₂-Fe₃O₄ NPs at different temperatures.

Reference

1. M. Hasegawa, J.-i. Takano, H. Enozawa, Y. Kuwatani and M. Iyoda, *Tetrahedron Lett.*, 2004, **45**, 4109-4112.